Egypt. J. Chem. **Vol. 65**, No. 9 pp. 477 - 495 (2022)

Egyptian Journal of Chemistry

http://ejchem.journals.ekb.eg/

Cobalt (II), Nickel (II) and Copper (II) complexes of Tetradentate Schiff base ligands derived from 4-Nitro-O-phenylenediamine: Synthesis, Characterization, cyclic voltammetry and biological studies

Maurice Kuate[1,3], Evans Mainsah Ngandung[2], Francis A. Ngounoue Kamga[1], Awawou G. Paboudam[1], Conde Asseng Mariam[3], Chancellin Nkepdep Pecheu[4], Tonle Kenfack Ignas[4] and Peter T. Ndifon[1]*

*[1]. Coordination Chemistry Laboratory, Department of Inorganic Chemistry, Faculty of Science, University of Yaoundé 1, P.O. Box 812 Yaoundé Cameroon. * [2]. Department of Chemistry, Faculty of Science, University of Buea, Cameroon [3]. Department of Chemistry, Faculty of Science, University of Douala, Cameroon [4]. Department of Chemistry, Faculty of Science, University of Dschang, Cameroon*

Abstract

Two tetradentate Schiff base ligands, (N,N"-bis((2-hydroxy-1-phenyl)methylidene)- 4-nitrophenyl-1,2-diamine (H_2L_1) and N,N'-bis((2-hydroxy-1-naphthyl)methylidene)-4-nitrophenyl-1,2-diamine (H_2L_2)) have been synthesized by the condensation of 4-nitro-orthophenylenediamine with 2-hydroxy-1-naphthaldehyde and salicylaldehyde respectively in absolute ethanol and reacted with Co(II), Ni(II) and Cu(II) salts to form the corresponding complexes. The compounds were characterized by UV-vis., FT-IR, ^{1}H NMR, ^{13}C NMR, ESI-mass spectra, elemental analysis, and molar conductance measurements. The ligands were found to be tetradentate, coordinating to the metal ions through the azomethine nitrogen and oxygen atoms of phenol and naphthol and the sulphur atoms of thiophenol groups. Conductance measurements shows that these compounds are molecular. Cyclic voltammetry studies shows that the Co(III)/Co(II) and Ni(III)/Ni(II) redox systems are quasi-reversible involving a mono electronic transfer while Cu(III)/Cu(II) is irreversible. *In vitro* antimicrobial screening against five bacterial strains (*Escherichia coli*, *Staphylococcus aureus*, *Pseudomonas aeruginosa*, *Enterococcus faecalis*, *Proteus mirabilis* and five fungal strains (*Candida albicans*, *Candida glabrata*, *Candida tropicalis*, *Candida krusei*, *Candida parapsilosis)*, shows that some of the compounds exhibited moderate antibacterial and antifungal activities compared to the reference drugs. Antioxidant studies reveal that the complexes are more potent than the ligands to eliminate free radicals.

Keywords: Tetradentate Schiff base ligands, 4-nitro-orthophenylenediamine, 2-hydroxy-1-naphthaldehyde, metal complexes, cyclic voltammetry, antimicrobial activity

1. Introduction

Schiff bases are considered as privileged ligands because they easily form stable complexes with most transition metal ions. Their complexes have been extensively studied because of the ease with which they are synthesized, their stability under certain oxidation and reduction conditions as well as diversity and flexibility in structures [1-3]. They possess diverse properties, thus potential applications as catalysts [4, 5], therapeutic agents and biological models [6-9]. They have been shown to possess a wide variety of antimicrobial activity against pathogenic bacteria and fungi as well as antioxidants, antiviral and antitumor agents [7-11].

Schiff bases are generally monodentate, bidentate [12, 13], tridentate [14] or tetradentate [15-17] ligands, capable of forming stable complexes with many transition metal ions. Tetradentate Schiff base ligands of N_2O_2 donor atoms, derived from the condensation reactions of diamines and the corresponding aldehydes or ketones are well known [18, 19]. Many complexes of tridentate and tetradentate Schiff base ligands with metal ions have been investigated as models for certain DNA binding and cleavage studies [17-20]. 2-hydroxy-1-naphthaldehyde and salicylaldehyde were used to form many tetradentate Schiff base ligands with amino acid but their electrochemical study and biological properties where not investigated [21].

Our group has recently embarked on studies on cyclic voltammetry and the biological activities of heterocyclic tridentate Schiff base complexes [22-24]. In continuation of our studies on metal complexes of heterocyclic Schiff base ligands, we report herein, the synthesis and electrochemical

*Corresponding author e-mail: pndifon@facsciences-uy1.cm
Received date 30 June 2021; revised date 31 December 2021; accepted date 27 January 2022
DOI: 10.21608/EJCHEM.2022.82313.4087

studies of Cobalt(II), Nickel(II) and Copper(II) complexes of Tetradentate Schiff-base ligands derived from 4-nitro-orthophenylenediamine with 2-hydroxy-1-naphthaldehyde and salicylaldehyde and the evaluation their antioxidant and antimicrobial properties.

2. Experimental

2.1. Materials and Methods

All reagents and solvents were obtained from commercial sources (Sigma and Across Organic) and used without further purification. Microanalyses (C, H and N) data were obtained using a Perkin-Elmer model 240C elemental analyzer. Infrared spectra were recorded using a KBr disk on an ALPHA-P spectrometer in the 4000- 400 cm^{-1} region. Electronic spectra were recorded in chloroform using UV-Vis spectrophotometer spectro Scan 80D in 300-800 nm range. ^{1}H-NMR for the ligands were recorded on a Bruker AMX 300 spectrometer operating at 300.13 MHz. High-resolution mass spectra were obtained using a Waters Micromass LCT Premier, Mass Spectrometer in Electron Spray ionization ESI mode. Cyclic voltammograms were recorded on a µAUTOLAB type III potentiostat/galvanostat and experiments were conducted under dry nitrogen conditions using a conventional three-electrode cell system. A glassy carbon electrode was used as the working electrode; Ag/AgCl and platinum were employed as the reference and auxiliary electrodes respectively. A 0.05M solution of H_2SO_4 was used as the supporting electrolyte. All electrochemical measurements were carried out in DMF solutions containing 10^{-3} M of either the ligand or its metal complexes. These solutions were degassed using a current of N_2 gas prior to any recording of cyclic voltammograms while maintaining them under inert atmosphere.

2.2. Synthesis of Schiff base ligands

2.2.1. Synthesis of N,N'-bis((2-hydroxy-1-phenyl)methylidene)-4-nitrophenyl-1,2-diamine (H_2L_1)

The Schiff base H_2L_1 was prepared by the condensation reaction between salicylaldehyde (1.148 g, 9.4 mmol) and 4-nitro-*o*-phenylenediamine (0.721 g, 4.7 mmol) in 30 mL of ethanol and heating the mixture under reflux for 4 hours as shown in scheme 1. The resulting solution was evaporated to about half the volume of the solvent to obtain a yellow precipitate which was filtered, washed several times with ethanol and air-dried. Yield: 68.77% (1.168 g); m.p 160°C; elemental analysis for $C_{20}H_{15}N_3O_4$ %Found(calc): C, 66.57(66.48); H, 4.21(4.18); and N, 11.68(11.63). ESI-MS in MeOH: *m/z* 360.4 $[M-H]^+$.

2.2.2. Synthesis of N,N'-bis((2-hydroxy-1-naphthyl)methylidene)-4-nitrophenyl-1,2-diamine (H_2L_2)

The Schiff base H_2L_2 was prepared by a condensation reaction between 2-hydroxylnaphthalaldehyde (0.86 g, 5.00 mmol) and 4-nitro-*o*-phenylenediamine (0.38 g, 2.50 mmol) in 30 mL of ethanol and heating the mixture under reflux for 4 hours as shown in scheme 1. The resulting solution was evaporated to about half the volume of the solvent. The yellow-orange product was filtered, washed several times with ethanol and air-dried. Yield: 64.2% (0.766 g); m.p 120°C; elemental analysis for $C_{28}H_{19}N_3O_4$ %Found(calc): C, 73.05(72.88); H, 4.26(4.15); and N, 8.98(9.11). ESI-MS in MeOH: *m/z* 496.2 $[M+Cl]^+$.

2.2.3. Synthesis of the complexes

All complexes were synthesized using a procedure reported elsewhere [25]. The metal nitrate hydrate (1.00 mmol), was dissolved in 10 mL methanol and added drop-wise to a vigorously stirring methanolic solution (1.00 mmol) of the ligand (H_2L_1 and H_2L_2). The resulting solution was stirred under reflux for 2 hours and cooled. The resulting coloured precipitates were filtered, washed thoroughly with ethanol and air-dried at room temperature.

2.3. Cyclic Voltammetry

Cyclic voltammetry studies were carried out using µAUTOLAB type III potentiostat/galvanostat and a three-electrode cell made up of glassy carbon as the working electrode, which was polished with an Al_2O_3 suspension prior to every experiment, Ag/AgCl and Pt foil used as pseudo reference and counter electrodes respectively. Solutions of the Schiff base ligands and complexes (1.0×10^{-3} M) in DMF, with sulfuric acid (0.05 M) as supporting electrolyte were purged of oxygen by bubbling through, dry nitrogen gas for 15 minutes and then blanketed with the same gas during the experiments. All compounds were investigated at room temperature. The voltammograms were recorded with a potential scan rate of 100 $mV\cdot s^{-1}$.

2.4. In vitro Antioxidant activity

Schiff bases H_2L_1, H_2L_2 and their complexes were tested for *in vitro* antioxidant activities using DPPH free radical scavenging assay [26, 27] with some modifications. Solutions of the ligands and their complexes at different concentrations (200, 100, 50, 25.5 and 12.25 µg/mL) were prepared in methanol. Different concentrations of 1mL of each sample and 540 µL of DPPH (0.08 mg/mL) solution were measured into different test tubes and the mixture shaken vigorously for about 2-3 minutes. The contents of the test tubes were then incubated in the dark for 30 minutes at room temperature. A blank

DPPH solution without the sample, used for the baseline correction gave a strong absorption maximum at 517 nm (purple color with ε = 8.32 x $10^3 M^{-1}$ cm^{-1}). After incubation, the absorbance value for each sample was measured using a UV-visible spectrometer and the relative free radical scavenging effects was calculated using the formula:

$$\text{scavenging effect\%}) = \frac{[\text{Abs}_{Contol} - \text{Abs}_{Sample}]}{\text{Abs}_{Contol}} X\ 100, [28,29]$$

where **$Abs_{(control)}$**: absorbance of DPPH radical + DMF and **$Abs_{(Sample)}$:** absorbance of DPPH radical + sample [test samples/ standard]. All the analyses were made in triplicate and values were compared with those of Trolox used as standard.

2.5. Antimicrobial study

The synthesized compounds were screened for *in vitro* antibacterial and antifungal activity against the bacterial strains: *Escherichia coli, Staphylococcus aureus, Pseudomonas aeruginosa, Enterococcus faecalis, Proteus mirabilis* and fungi species: *Candida albicans, Candida glabrata, Candida tropicalis, Candida krusei, and Candida parapsilosis.* Ciprofloxacine and Ketoconazole (at 1 mg/ml in DMSO) were used as reference drugs for bacteria and fungi respectively.

2.5.1. Determination of the diameters of zone of inhibition

The diameters of the zone of inhibition of the synthesized compounds were determined using the agar well diffusion method [30]. The stock solutions (1 mg/mL) of the compounds were prepared in DMSO at 37°C and incubated for 24 hours and 48 hours for bacteria and yeasts respectively. The antimicrobial activities were assessed by measuring the diameter of the zone of inhibition of the bacterial growth around every well with a ruler following two axes. Three determinations were made for every product tested.

2.5.2. Minimum inhibitory concentration

The minimum inhibitory concentrations (MIC) were determined by the method of micro dilution in the 96-well micro titer plates for the bacterial species [31]. The quantitative antibacterial or antifungal activities of the test compounds were evaluated using micro dilution broth method [32]. Two-fold serial dilutions of the compounds were prepared in 96-well micro titer plates using sterile nutrient broth as diluent. The plates were inoculated with 100 µL bacterial or fungal suspensions containing $1.5x10^8$ colony-forming units (CFU) [33] and incubated at 37 °C for 48 hours for fungi and 24 hours for bacteria.

3. RESULTS AND DISCUSSION

The physical properties and analytical data of the compounds are summarized in Table 1. The Schiff base ligands were prepared by the condensation reaction in absolute ethanol, under reflux between 4-nitro-*o*-phenylenediamine and salicylaldehyde for H_2L_1 and 2-hydroxylnaphthalaldehyde for H_2L_2 as shown in Scheme 1. The Schiff base ligands obtained as powders, melted at 177 and 120 °C for H_2L_1 and H_2L_2 respectively and were soluble in methanol, DMF and DMSO. The yellowish color of the Schiff bases is indicative of the formation of the imine (-C=N-) group.

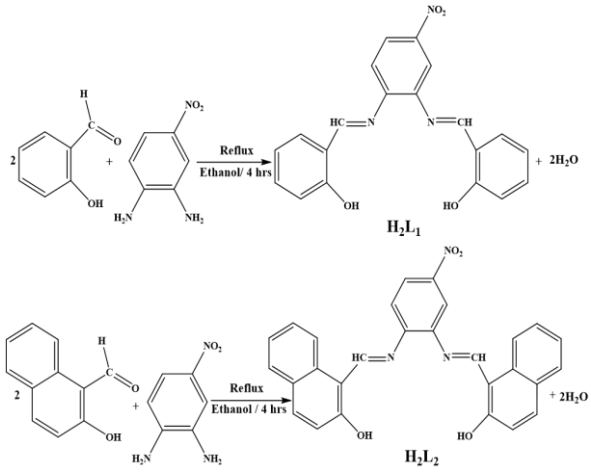

Scheme 1. Synthesis of the Schiff bases ligands H_2L_1 and H_2L_2

Microanalysis results of the compounds agree with the expected values, thus confirming the purity of the compounds and the 1:1 reaction ratio for metal ion/ligand during the formation of the complexes. The low molar conductivities of the synthesized compounds in DMSO suggest the molecular nature of all the complexes.

3.1. Infrared study

The important spectral bands of the ligands (H_2L_1 and H_2L_2) and their corresponding metal complexes are presented in Table 2. In the spectra of the ligands (Figure 1), the strong and broad bands at 3455–3385 cm^{-1} and 3470–4347 cm^{-1} are attributed to $_{(O-H)}$ of phenol respectively [34-36]. The strong bands at 1617 and 1633 cm^{-1} are assigned to the $\nu_{(C=N)}$ azomethine group of H_2L_1 and H_2L_2 respectively [36-38].

Also, the strong and medium bands which appear in the spectrum of each ligand at 1573 cm^{-1} and 1345-1296 cm^{-1} correspond to aromatic nitro-group $_{(NO_2)assym}$ and $\nu_{(NO_2)sym}$ respectively. The strong bands at 1200-1160 cm^{-1} and 808-745 cm^{-1} are assigned to the $\nu_{(C-O)sym}$ and $\nu_{(C-O)assym}$ respectively in H_2L_1 and H_2L_2 ligands [38].

The band characteristic of the azomethine group $\nu_{(C=N)}$ at 1613 and 1633 cm^{-1} in the free ligands H_2L_1 and H_2L_2 respectively are shifted to lower wave

number in all the complexes suggesting the involvement of the azomethine nitrogen atom in coordination with the metal ions [36-38]. The absence of the medium bands in the 3455–3385 cm^{-1} and 3470–4347 cm^{-1} ranges associated to $_{(O-H)}$ of phenolic group also suggested the involvement of phenolic oxygen in coordination after deprotonation [36-38].

Thus, the ligands act as tetradentate chelating compounds coordinating to the metal ions through the two oxygen atoms of the phenol moiety and the two azomethine nitrogen atoms [38]. In all the complexes, the new bands observed at 573- 546 cm^{-1} and 515–490 cm^{-1} can be attributed to the ν_{M-O} and ν_{M-N} modes respectively for H_2L_1 complexes and at 508- 504 cm^{-1} and 494-426 cm^{-1} for H_2L_2 complexes.

Table 1. Physical properties and analytical data of the Schiff bases and complexes

Compounds	Colour	Yield (%)	Melting point	Molar mass ($g.mol^{-1}$)	%Found(calculated)			Λ_m (Ω^{-1} cm^2 mol^{-1})
					C	H	N	
H_2L_1	Yellow	68.8	177	361.4	66.57 (66.48)	4.21 (4.18)	11.68 (11.63)	0.13
CuL_1	Brown	75.1	>360	485.9	50.42 (49.44)	3.49 (2.90)	12.34 (11.53)	2.40
CoL_1	Dark- Pink	69.3	>360	418.3	57. 07 (57.43)	3.24 (3.13)	10.11 (10.05)	0.87
NiL_1	Red	65.5	>360	481.0	50.11 (49.94)	3.60 (2.93)	11.91 (11.65)	1.88
H_2L_2	Yellow-orange	64.2	120	461.1	73.05 (72.94)	4.21 (4.18)	11.68 (11.63)	1.13
CuL_2	brown	65.6	>360	686.02	57.60 (57.39)	3.47 (3.10)	9.37 (9.56)	2.40
CoL_2	Dark- Pink	74.2	>360	581.4	57.07 (57.84)	3.24 (3.12)	9.47 (9.64)	0.87
NiL_2	Red	70.5	>360	5817.17	57.41 (57.87)	3.48 (3.12)	9.89 (9.64)	1.20

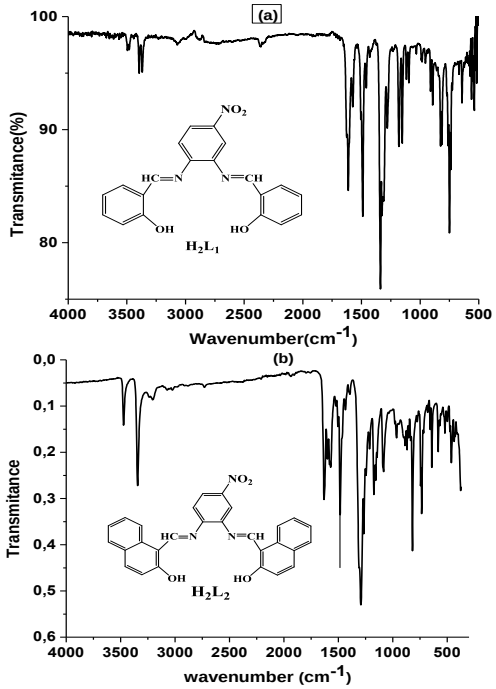

Figure 1. IR spectra of Schiff bases H_2L_1 (a) and H_2L_2 (b)

3.2. ^{1}H NMR spectral analysis

The ^{1}H NMR spectra of the Schiff bases H_2L_1 and H_2L_2 in DMSO are presented in Figure 2. The singlet (s, 2H) at 11.84 and 14.53 ppm correspond to the phenolic $\boldsymbol{\delta}_{(O-H)}$ proton. While the azomethine proton $\boldsymbol{\delta}_{(H-C=N)}$ appeared as a singlet (s, 2H) at 8.98 and 9.68 respectively for H_2L_1 and H_2L_2 [28-30]. The peak at 7.86-6.42ppm (m, 11H) and 8.53 – 6.47ppm (m, 15H) are attributed to the aromatic proton $\boldsymbol{\delta}_{(Ar-H)}$ of H_2L_1 and H_2L_2 respectively [30-32]. The appearance of the azomethine proton $\boldsymbol{\delta}_{(H-C=N)}$ and phenolic $\boldsymbol{\delta}_{(O-H)}$ proton confirm the tetradentate nature of the Schiff bases (H_2L_1 and H_2L_2).

When the spectra of ligands and complexes are compared as summarized in Table 3, it was observed that the peaks at 11.84 and 14.53 in the ligands attributed to the OH protons are absent in the complexes, confirming the deprotonation of the OH during complexation, earlier suggested from IR data. The azomethine protons are shifted up field, confirming the involvement of the azomethine nitrogen in coordination [39-41].

Table 2. IR data of ligands (H_2L_1 and H_2L_2) and their complexes

Compounds	$\nu_{C=N}$	ν_{NO2}	ν_{C-O}	ν_{C-O} *asym*	ν_{O-H}	ν_{M-N}	ν_{M-O}
H_2L_1	1613	1340	1175	826-750	3455-3385	/	/
CuL_1	1604	1330	1182	827-760	/	549	567
CoL_1	1602	1335	1198	831-756	/	539	570
NiL_1	1604	1337	1201	834-760	/	561	592
H_2L_2	1633	1296	1173	818-739	3470-3347	/	/
CuL_2	1614	1320	1195	827-741	/	495	555
CoL_2	1614	1327	1245	821-746	/	504	567
NiL_2	1615	1333	1198	824-742	/	502	572

Table 3. ^{1}H-NMR data of the Schiff base and its corresponding complexes

Compounds	$\delta_{(O-H)}$	$\delta(_{N=C^-H)}$	$\delta(_{Ar-H)}$
H_2L_1	11.84 ppm (s, 2H)	8.98ppm (s, 2H)	7.86 - 6.42 (m, 11H)
CuL_1	/	8.75ppm (d, 2H)	7.45 - 4.12 (m, 11H)
CoL_1	/	8.70ppm (s, 2H)	7.62 - 5.04 (m, 11H)
NiL_1	/	8.95ppm (s, 2H)	7.78 - 5.84 (m, 7H)
H_2L_2	14.53 ppm (s, 2H)	9.68ppm (s, 2H)	8.58 - 6.60 (m, 15H)
CuL_2	/	8.86ppm (s, 2H)	8.01 - 5.72 (m, 15H)
CoL_2	/	9.57ppm (s, 2H)	7.85 - 5.22 (m, 15H)
NiL_2	/	8.69ppm (s, 2H)	7.83 - 6.33 (m, 15H)

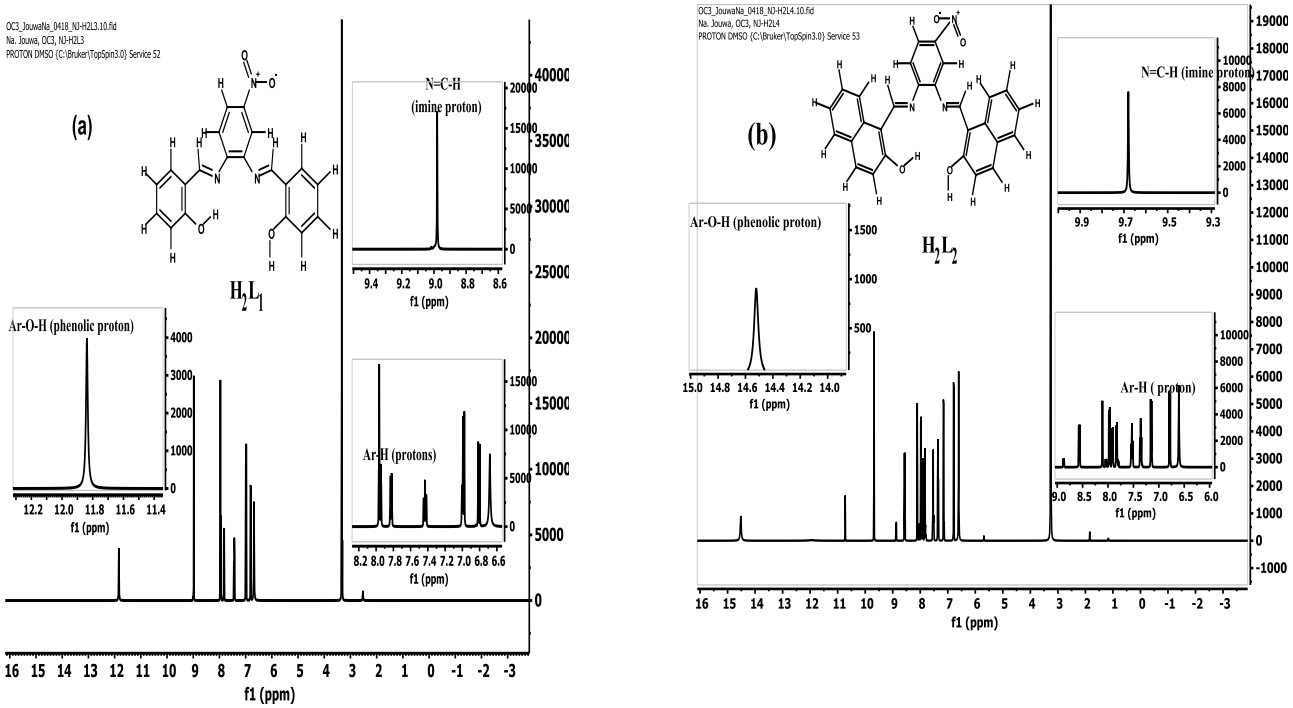

Figure 2. ^{1}H-NMR spectra of Schiff base ligand H_2L_1 (a) and H_2L_2 (b)

3.3 ^{13}C NMR spectral analysis

The ^{13}C NMR spectra of Schiff bases H_2L_1 and H_2L_2 (Figure 3) shows signals at 163.07 ppm and 163.60 ppm respectively, attributed to azomethine carbon **δ**(HC=N-) [39-41]. The peaks at 160.1 ppm and 161.33 ppm for H_2L_1 and H_2L_2 are assigned to phenolic carbon **δ**(C–OH). Three other signals observed at 150.46 ppm, 136.64 and 134.25 ppm in H_2L_3 spectrum and 149.98 ppm, 136.98 ppm ad 136.08 ppm in H_2L_4 spectrum and to the aromatic carbon bonded to the azomethine nitrogen **δ**(-C-N=) [39-41], The spectra also show other peaks between 133 and 110 ppm attributed to aromatic carbons [39-41].

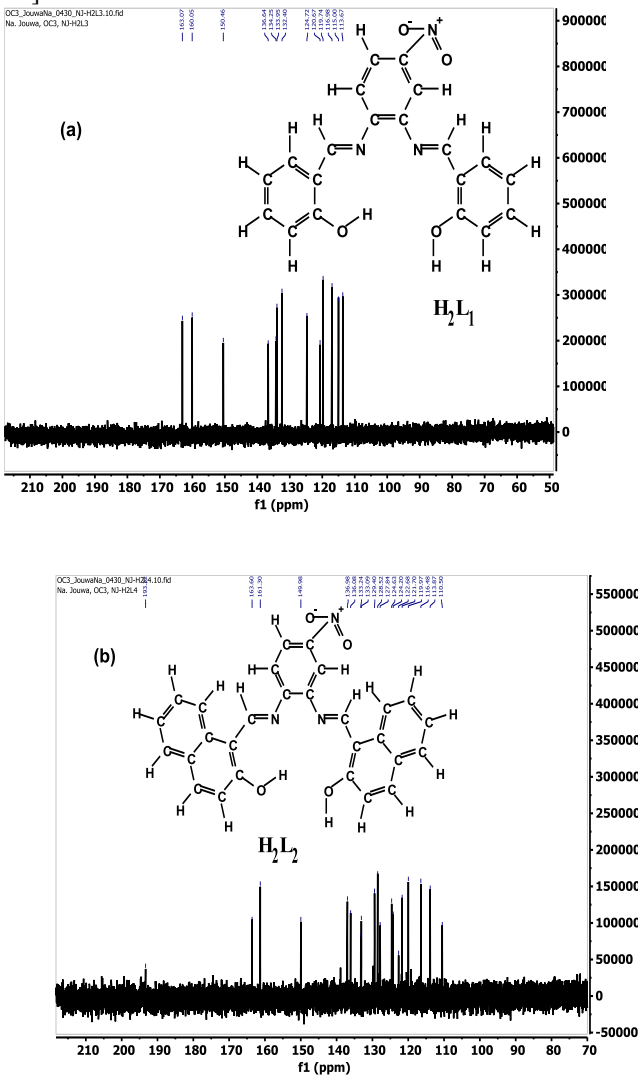

Figure 3. ^{13}C-NMR spectra of the Schiff base ligand H_2L_1 (a) and H_2L_2 (b)

3.4. Mass spectra

The mass spectra (MS) of Schiff bases shows the molecular weight and fragmentation pattern. The molecular ion peak was observed at m/z 360.4 for H_2L_1 and m/z 496.2 for H_2L_2, confirming molecular formulae of ($C_{20}H_{15}N_3O_4$) and ($C_{28}H_{19}N_3O_4$) respectively [39-41]. These values are in agreement with the calculated $[M\text{-}H]^+$ and $[M + Cl]^+$ values for H_2L_1 and H_2L_2 respectively, corresponding to the molecular weight of 361.4 and 461.48 for H_2L_1 and m/z 496.2 for H_2L_2 respectively [39-41]. The mass spectra of H_2L_1 and H_2L_2 are shown in Figure 4.

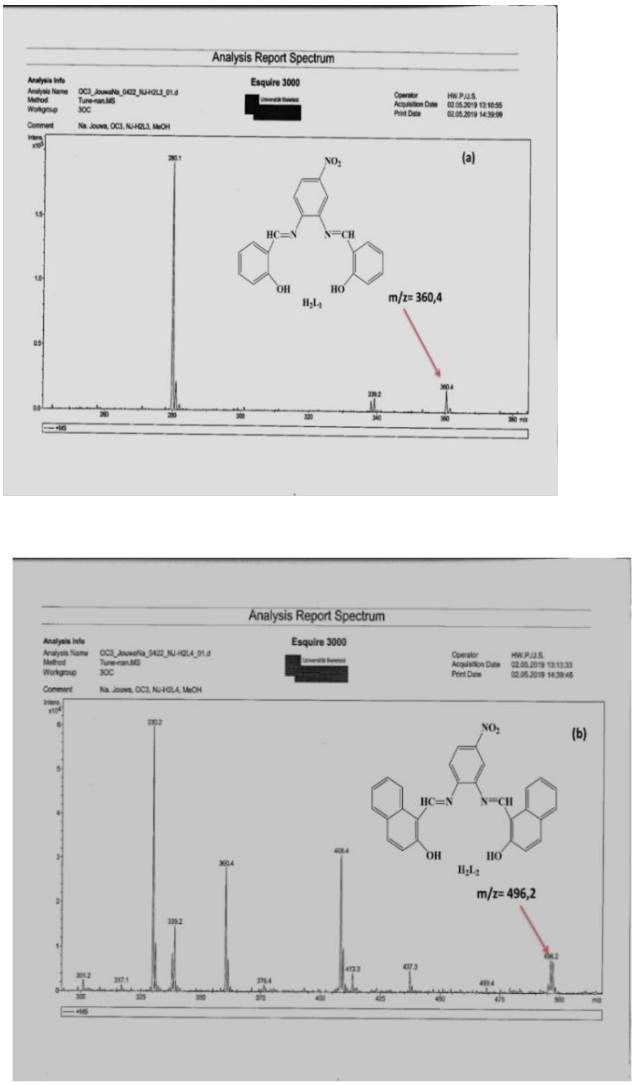

Figure 4. Mass spectra of the Schiff base ligand H_2L_1 (a) and H_2L_2 (b).

3.5. Electronic Spectra

The UV-Visible spectra of the compounds are presented in Figures 5 and 6 while band assignments and the proposed geometry are listed in Table 4. The spectra of H_2L_1 and H_2L_2 exhibited higher intense bands at 320 nm (31250 cm^{-1}) and 318 nm (31446 cm^{-1}) assigned to $\pi \rightarrow \pi^*$ transition, and at 391 nm (25575 cm^{-1}) and 395 nm (25316 cm^{-1}) assigned to $n \rightarrow \pi^*$ transition [39-41]. The entire bands in the

spectrum of the Schiff base are shifted in the spectra of some complexes and disappear in the others due to coordination. The spectra of CoL_1 and CoL_2 complexes shows an absorption band at 520-505 nm (19 801 cm^{-1}) and 606-603 nm (16 501 cm^{-1}) suggesting the $^4T_1(P) \rightarrow {}^4T_2(F)$ and $^4T_1(F) \rightarrow {}^4A_2(F)$ transition typically for tetrahedral environments [39,42]. The spectra of CuL_1 and CuL_2 complexes show absorption bands at 451 nm (22172 cm^{-1}) and 453 nm (22075 cm^{-1}) attributed to $^2B_{1g} \rightarrow {}^2A_{1g}$ transition of square planar geometry around Cu(II) ion [19, 41] as expected from the nature of the ligands and the resulting steric effects. The spectrum of NiL_1 show absorption bands at 484 nm (20661 cm^{-1}) and 597 nm (16750 cm^{-1}) attributed to $^3T_1(P) \rightarrow {}^3A_2(F)$ and $^3T_1(F) \rightarrow {}^3A_2(F)$ transition of tetrahedral geometry. [39-42].

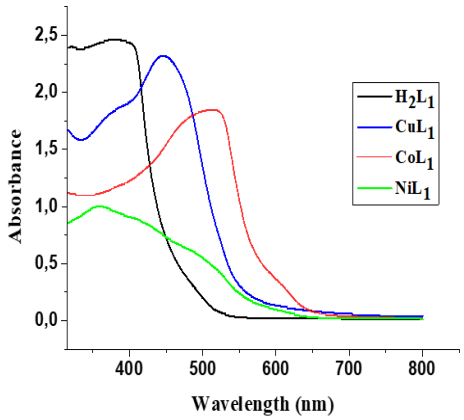

Figure 5. Electronic spectra of ligand H_2L_1 and its Corresponding complexes

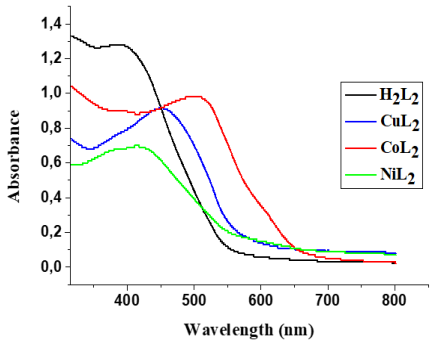

Figure 6. Electronic spectra of ligand H_2L_2 and its corresponding complexes

3.6. Thermogravimetric analysis of the complexes

The differential and thermo gravimetric analyses of complexes were determined under a nitrogen gas inert atmosphere in the range 10 and 700 °C. The thermograms and data obtained are shown in Figure 7 and summarized in Table 5. The thermal decomposition curves of CoL_1 and NiL_1 complexes showed single step decomposition corresponding to the loss of a part of ligand at 273 °C (found: 53.28; calc: 53.61) and 280 °C (found: 50.67; calc: 50.14) respectively. The corresponding residue are CoO and NiO. The thermal decomposition curve of the CuL_1 complex showed two steps decomposition. The first step at 280-430 °C corresponding to a loss of one mole of ligand (found: 64.81; calc: 65.24). While the second step occurred below 330 °C (found: 9.49; calc: 9.46) corresponding to the loss of one molecule of NO_2 gas and the residue is CuO (found: 25.70; calc: 25.84) [36-39].

The thermogram for CuL_2 present single step decomposition between 140- 430 °C corresponding to the loss of one mole of ligand and water molecule (found: 77.83; calc: 77.89). The thermogram for NiL_2 also shows a single step decomposition between 310-510 °C attributed to the loss of one mole of ligand and water molecule (found: 73.14; calc: 73.18). The single step decomposition observed for CoL_2 complex at 180- 430 °C, corresponds to the loss of one molecule of ligand (found: 61.16; calc: 61.21) [36-39]. In all of these case, the residue appear as metal oxide (CuO, NiO and CoO).

Analytical result suggested that the Schiff base ligands (H_2L_1 and H_2L_2) coordinated to the metal ions via the azomethine nitrogen and phenolic oxygen in tetradentate mode. Electronic spectral data suggest tetrahedral geometry for Co(II) and Ni(II) complexes and square planar in geometry for Cu(II) complex [19, 41].

3.7. Cyclic voltammetry study

The electrochemical behavior of Schiff bases and their corresponding Co(II), Ni(II) and Cu(II) complexes were investigated in DMF between -1.5 V to 1.5 V and a scan rate of 100 $mV.s^{-1}$.

3.7.1. Cyclic voltammetry study of the Schiff bases

The cyclic voltammograms of the ligand H_2L_1 (Fig. 9) shows two anodic waves respectively at E_{pa1}= 0.333 V ($1.397x10^{-5}$A) and corresponding to a two-electron oxidation processes [42]. For the return sweep, two reduction waves were observed at -0.087 V and -1.177 V. The first wave observed at E_{pc1}= 0.087 V ($1.137x10^{-5}$A) is attributed to the reduction of the nitro group [42, 43]. And the second wave observed at E_{pc2}= -1.177 V ($6.329x10^{-5}$A) corresponds to the reduction processes of the azomethine moiety [42, 43]. The electron transfer process in the Schiff base H_2L_1 is described by scheme 2.

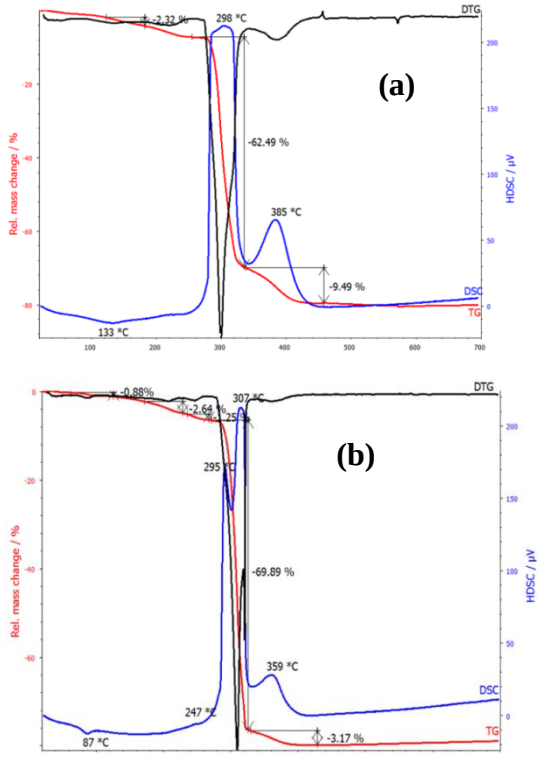

Figure 7. Thermogramms of CuL_1 (a) and CuL_2 (b)

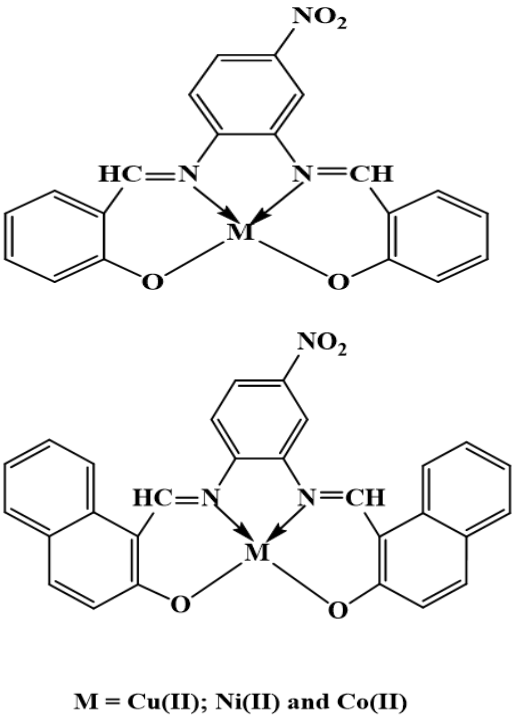

Figure 8. Proposed structures of metal complexes

The cyclic voltammograms of the ligand H_2L_2 (Fig. 5) shows three anodic waves at 0.572 V, 0.784 V and 1.223 V corresponding to the successive oxidation of the nitro group and Schiff base [42, 43]. For the return sweep, three reduction waves were observed at 0.653 V, -0.077 V and -0.512 V. corresponding to the reduction of the nitro group (scheme 3) [42] and the two-electron successive reduction processes of the oxidized form of the azomethine moiety [42, 43].

The two-electron successive transfer process in H_2L_2 is represented in scheme 4.

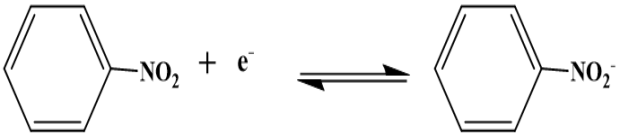

Scheme 3. Oxidation processes of nitro group

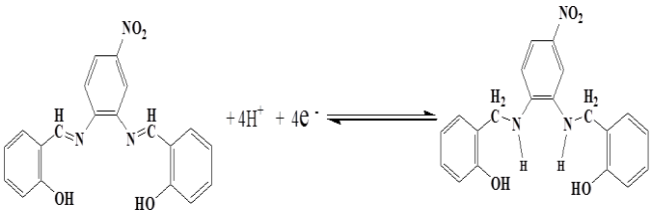

Scheme 2. Electron transfer process in Schiff base H_2L_1

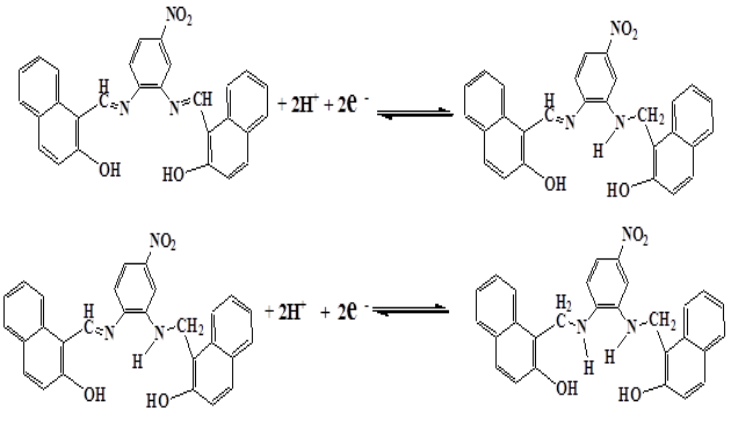

Scheme 4. Successive two-electron transfer processes in Schiff base H_2L_2

3.8. Cyclic voltammetry studies of complexes

Knowledge of electrochemical redox processes of free ligands is important to properly assign the electron transfer processes of corresponding complexes [24, 25]. The voltammograms show anodic wave at nearly the same potential as the corresponding peaks in the voltammograms of the free ligands. Analysis of the recorded voltammograms of the complexes indicates that the obtained redox potentials depend on the nature of substituents on the ligand.

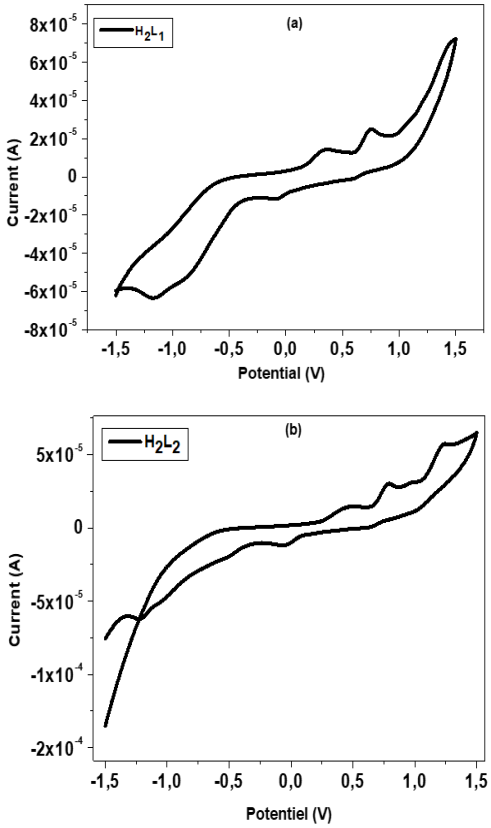

Figure 9. Cyclic voltammogram of the Schiff bases H_2L_1 (a) and H_2L_2 (b)

3.8.1. Cyclic voltammetry studies of complexes of H_2L_1 Schiff base ligand

Cyclic voltammograms of complexes of H_2L_1 Schiff base ligand, displaying two oxidation peaks are presented in Figure 10. The intense oxidation peak at 0.024 V ($8.425x10^{-5}$A), 0.433 V ($1.029x10^{-5}$A) or 0.421V($1.519x10^{-5}$A) with the associated reduction peaks at -0.483 V ($-4.123x10^{-5}$A), -0.224 V ($-1.013x10^{-5}$A) or -0.287 V ($-1.540x10^{-5}$A) correspond to the Cu(III)/Cu(II), Co(III)/Co(II) or Ni(III)/Ni(II) couples respectively [42- 48] while the weak peaks are attributed to the oxidation and reduction of the ligand moiety [45-48].

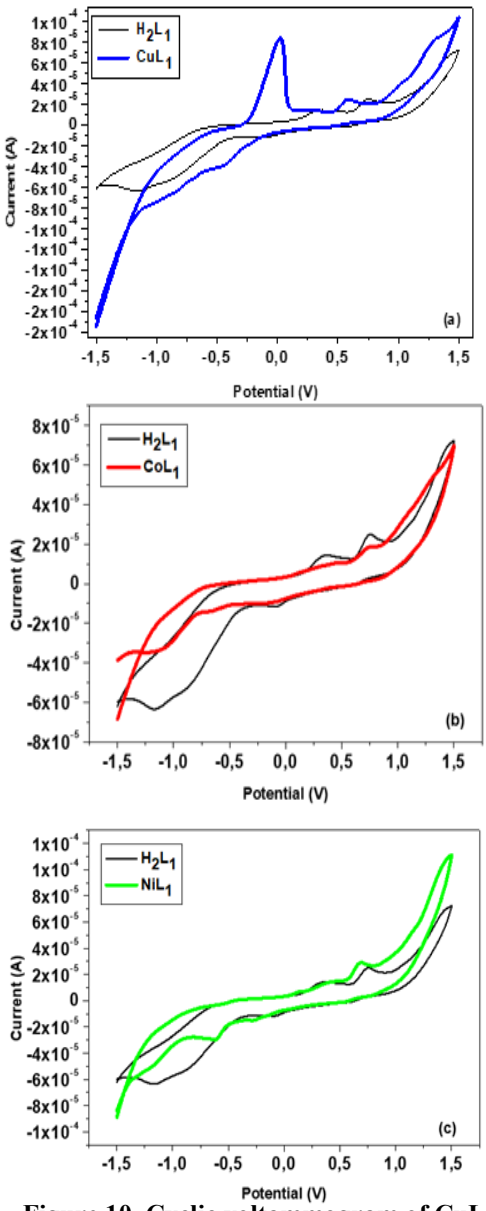

Figure 10. Cyclic voltammogram of CuL_1 (a), CoL_1 (b) and NiL_1 (c) complexes

3.8.2 Cyclic voltammetry studies of complexes of H_2L_2 Schiff base ligand

Cyclic voltammograms of complexes of H_2L_2 Schiff base ligand displaying two oxidation peaks are presented in Figure 11. The intense oxidation peak at 0.083 V ($6.900x10^{-5}$A), -0.136 V ($0.749x10^{-5}$A) or 0.447 V ($1.069x10^{-5}$A) with associated reduction peak at -0.324 V ($-1.901x10^{-5}$A), -0.628 V ($-1.989x10^{-5}$A) and -0.124 V ($-9.172x10^{-6}$A) corresponds to Cu(III)/Cu(II), Co(III)/Co(II) or Ni(III)/Ni(II) couple respectively[42- 48] while the less intense peaks are attributed to the oxidation and reduction of the H_2L_2 ligand moiety [45-48].

Table 4. Electronic spectral data of the ligand and their corresponding complexes

Compounds	λ(nm) and ν(cm^{-1})	Assignments	Suggested structures
H_2L_1	320 nm (31 250 cm^{-1})	π→ π*	/
	491 nm (25 575 cm^{-1})	*n*→ π*	/
CuL_1	318 nm (31 446 cm^{-1})	H_2L_3 chromophore (π→ π*)	Square planar
	386 nm (25 906 cm^{-1})	Charge transfer(L→M)	
	451 nm (22 172 cm^{-1})	$^2B_{1g}$→$^2A_{1g}$	
CoL_1	317 nm (31 545 cm^{-1})	H_2L_3 chromophore (π→ π*)	Tetrahedral
	395 nm (25 316 cm^{-1})	Charge transfer(L→M)	
	520 nm (19 230 cm^{-1})	$^4T_1(P)$ → $^4T_2(F)$	
	603 nm (16 583 cm^{-1})	$^4T_1(F)$→ $^4A_2(F)$	
NiL_1	355 nm (28 169 cm^{-1})	H_2L_3 chromophore (π→ π*)	Tetrahedral
	406 nm (24 630 cm^{-1})	Charge transfer(L→M)	
	484 nm (20 661 cm^{-1})	$^3T_1(P)$ → $^3A_2(F)$	
	597 nm (16 750 cm^{-1})	$^3T_1(F)$→ $^3A_2(F)$	
H_2L_2	318 nm (31 446 cm^{-1})	π→ π*	/
	495 nm (25 316 cm^{-1})	*n*→ π*	/
CuL_2	316 nm (31 645 cm^{-1})	H_2L_4 chromophore (π→ π*)	Square planar
	394 nm (25 380 cm^{-1})	Charge transfer(L→M)	
	453 nm (22 075 cm^{-1})	$^2B_{1g}$→$^2A_{1g}$	
CoL_2	316 nm (31 645 cm^{-1})	H_2L_4 chromophore (π→ π*)	Tetrahedral
	397 nm (25 188 cm^{-1})	Charge transfer(L→M)	
	505 nm (19 801 cm^{-1})	$^4T_1(P)$ → $^4T_2(F)$	
	606 nm (16 501 cm^{-1})	$^4T_1(F)$→ $^4A_2(F)$	
NiL_2	421 nm (23 752 cm^{-1})	Charge transfer(L→M)	Tetrahedral
	592 nm (16 891 cm^{-1})	$^3T_1(F)$→ $^3A_2(F)$	

Table 5. Thermogravimetric analytical results for Cu(II), Co(II) and Ni(II) complexes of H_2L_1 and H_2L_2

Compounds	Step	TGA Temperature (°C)	DSC Temperature (°C)	Weight loss (%)		Fragment lost
				Found	Calc	
CuL_1	1	280	298 (Endothermic)	64.81	65.24	$C_{20}H_{16}N_2O_2$ (1 molecule of ligand)
	2	330	385 (Endothermic)	9.49	9.46	NO_2 (gas)
	Residue	>460		25.70	25.84	CuO,
CoL_1	1	273	360 (Endothermic)	53.28	53.61	$C_{13}H_{10}N_2O_2$ (1 molecule of ligand)
	Residue	>480		46.72	46.63	CoO;
NiL_1	Single	154-280	373 (Endothermic)	50.67	50.14	$C_{13}H_{12}N_3O_{2.75}$ (1 molecule of ligand+1/2H_2O)
	Residue	>440		49.33	49.06	NiO,
CuL_2	Single	140-430	307 (Endothermic)	77.83	77.89	$C_{28}H_{19}N_3O_4$ (1 molecule of ligand)
	Residue	>450		22.17	22.27	CuO
CoL_2	Single	180-430	365 (Endothermic)	61.16	61.21	$C_{18}H_{14}N_3O_{3.5}$ (1 molecule of ligand + 1/2H_2O)
	Residue	>450		38.84	38.98	CuO
NiL_2	Single	310-510	373 (Endothermic)	73.14	73.90	$C_{28}H_{20}N_3O_2$ (1 molecule of ligand)
	Residue	>520		26.86	26.57	NiO

3.8.3 Effect of the ligand on the electrochemical behaviors of the complexes

The napthyl group (compared to the phenyl) stabilizes the lower oxidation state of the metal ion because of the strong electron-withdrawing effect of the napthyl group [48, 49]. This effect lowers the electron density on the central metal ion as reduction centre which becomes more positive and thereby more easily reduced. Therefore, the electron-withdrawing group shifts the potential of the cathodic peak Epc to more positive values as can be seen from Table 6. The presence of electron-donating groups has the reverse effect [49]. Characteristic peak for the reduction of the imine group, shifts to more negative values with the decrease in the electron-donating ability of the substituents. Electron density on the copper ion in the complexes with phenyl groups is less and the metal coordination geometry may appear more distorted due to steric effects of the bulky napthyl group substituent [49].

3.9. Kinetic effect of the electrochemical process

In order to study the kinetics of the electrochemical processes, the redox systems of the complexes were investigated separately in the reduced potential range of -1.0 to 1.5 V at various scan rates (10 to 430 $mV.s^{-1}$) as shown in the voltammograms in Figure 12.

The peak to peak separation ΔEp increase with the scan rate and the ratio of cathodic to anodic (Ipa/Ipc) peak is near one for Co(II) and Ni(II) complexes, indicating the quasi-reversibility of the redox system. For the Cu(II) complexes, the ratio (Ipa/Ipc) is greater than one, indicate the irreversibility of the redox system. The respective one-electron transfer processes in the complexes are described by scheme 5

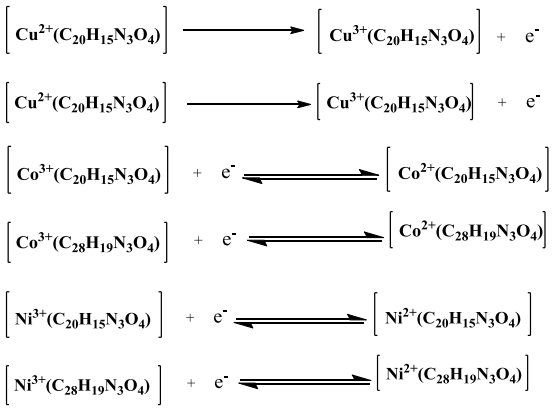

Scheme 5. Electron transfer process in complexes of H_2L_1 and H_2L_2 Schiff base ligand

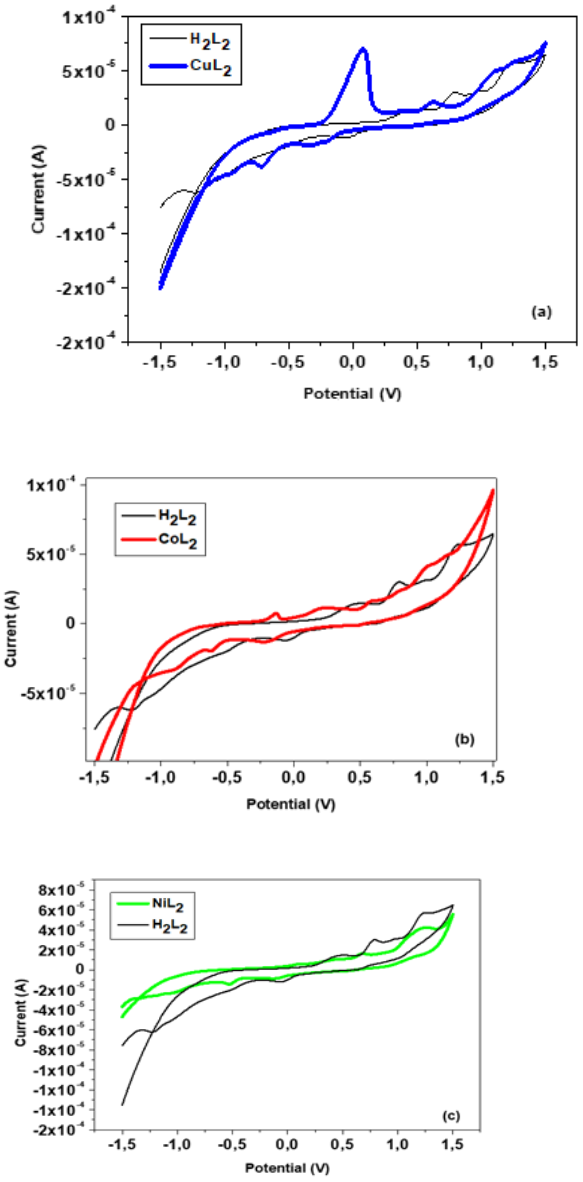

Figure 11. Cyclic voltammogram of CuL_2 (a), CoL_2 (b) and NiL_2 (c) complexes

3.10. Mechanism at the surface of the electrodes

The cyclic voltammograms of the ligands and their corresponding complexes, scanned 20 times at a scan rate 10 $mV.s^{-1}$ and superposed show all the peaks appearing in the same position for all the cycles, suggesting that there is no adsorption of the compound at the glassy carbon electrode surface [48]. Cyclic voltammograms of the ligands and their corresponding complexes, scanned at different scan rates (10 to 430 $mV.s^{-1}$), the peak current increases with an increase in the square root of the scan rates (Figures 12 and 13) suggesting that the electrode process is diffusion controlled [43,47]. The plot of

the cathodic peak potential versus the logarithm of scan rate shows a nonlinear relationship (Figure 14), indicating that even though the potential does not depend on the scan rate, the processes at the surface of the electrodes are slow [43, 47].

Table 6. Characteristic peaks obtained in voltammograms of complexes

Compounds	Epa_1 (V) Metal	Epc_1(V) Metal	Epa_2(V) Nitro group	Epa_1(V) imine	Epc(V) imine
CuL_1	0.024	-0.483	1.029	1.291	-0.851
CuL_2	0.083	-0.324	1.098	1.254	- 0.716
CoL_1	0.433	-0.145	0.735	1.073	- 1.070
CoL_2	0.229	-0.224	0.583	0.788	- 0.898
NiL_1	0.421	-0.287	0.687	1.123	- 1.183
NiL_2	0.447	-0.124	0.697	1.223	- 1.032

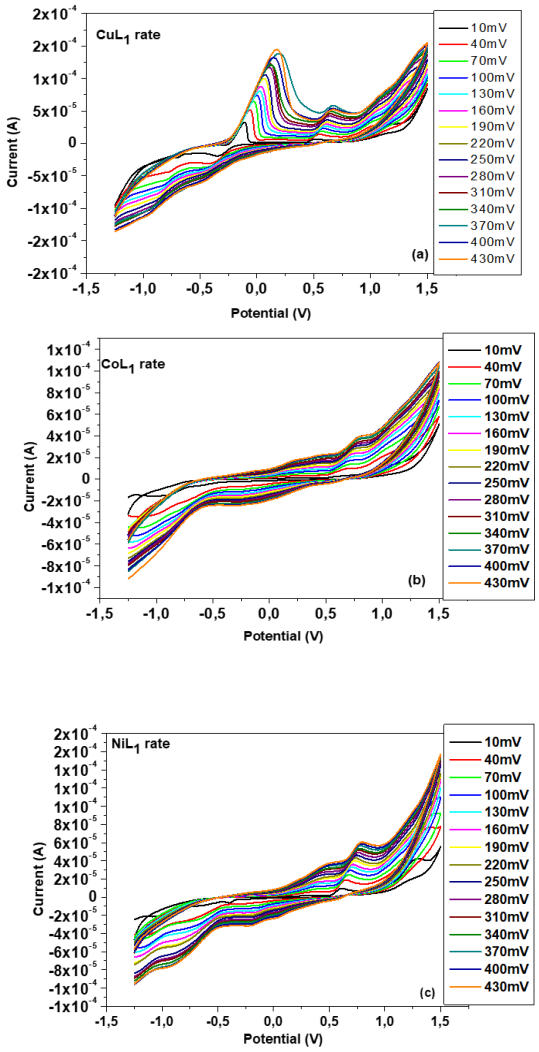

Figure 12. Variation of peak to peak separation with scan rate for (a) Cu(II)L_1, (b) Co(II)L_1 and (c) Ni(II)L_1 complexes

3.6. Biological study

3.6.1. Antimicrobial activity of the ligand and its metal complexes

The Schiff bases and their metal complexes were tested against five bacterial strains (*Escherichia coli, Staphylococcus aureus, Pseudomonas aeruginosa, Enterococcus faecalis, and Proteus mirabilis)* and five fungi *(Candida albicans, Candida glabrata, Candida tropicalis, Candida krusei, and Candida parapsilosis*) employing Ciprofloxacine and Ketoconazole as the reference material for bacterial and fungal studies respectively.

3.6.2. Determination of the Diameters of zone of the inhibition (DZI)

The diameters of the zone of inhibition of the ligand and their complexes were determined using agar well diffusion method [29]. The diameters of zone of inhibition on fungi and bacteria are summarized in Table 7 and 8 respectively, while Figure 15 and 16 are the histograms of the corresponding diameter of zone of inhibition.

The resulting data revealed that the compounds exhibited lower inhibition than ciprofloxacine and ketoconazole used as the reference materials. It was found that the Schiff bases (H_2L_1 and H_2L_2) did not show any antibacterial activity against the tested bacterial strains except *E. coli* on which H_2L_2 shows very low activity. All the metal complexes (M-L_1) are more active than the ligand H_2L_1 on *Escherichia coli, Staphylococcus aureus, Pseudomonas aeruginosa and Proteus mirabilis.* CoL_2 and NiL_2 complexes showed moderate antibacterial activity compared to the ligand H_2L_2 on *Escherichia coli* and *Pseudomonas aeruginosa.* Only CoL_2 complex showed higher antifungal activities than the ligand on *Candida krusei and Candida tropicalis.* This enhancement in the activity of the metal complexes compared to the ligand can be explained by the effect of chelation and the overtone's concept [38, 42, 48,]. On chelation, the polarity of the metal ion is reduced to a greater extent due to the overlap of the ligand orbital and partial sharing of the positive charge of the metal ion with donor groups. Furthermore, the delocalization of p-electrons over the whole chelate ring enhances the lipophilicity of the complex. This increased lipophilicity enhances the penetration of the

complexes into the lipid membranes thus increasing the bioavailability and hence, the biological activities [38, 42, 48]. Also the lipid membranes that surround the cell favours the passage of only liquid-solid materials due to lipo-solubility, thus contorts antimicrobial activity [38, 47].

3.6.3. Minimum inhibitory concentration (MIC)

After incubation at 37 °C, the lowest concentrations of the antimicrobials in which there was no visible growth of the microorganism represents their minimum inhibitory concentration and the results are presented in Tables 9.

Table 7. Diameters of the zone of inhibition on fungi

	Fungi				
Samples	***C. albicans***	***C. glabrata***	***C. krusei***	***C. tropicalis***	***C. parapsilosis***
H_2L_1	0.00 ± 0.00	0.00 ± 0.00	0.00 ± 0.00	**7.00 ± 0.40**	**8.50 ± 0.20**
CuL_1	0.00 ± 0.00	0.00 ± 0.00	0.00 ± 0.00	0.00 ± 0.00	0.00 ± 0.00
CoL_1	0.00 ± 0.00	0.00 ± 0.00	0.00 ± 0.00	0.00 ± 0.00	**6.00 ± 0.20**
NiL_1	0.00 ± 0.00	0.00 ± 0.00	0.00 ± 0.00	0.00 ± 0.00	0.00 ± 0.00
H_2L_2	0.00 ± 0.00	0.00 ± 0.00	**8.00 ± 0.20**	0.00 ± 0.00	0.00 ± 0.00
CuL_2	0.00 ± 0.00	0.00 ± 0.00	0.00 ± 0.00	0.00 ± 0.00	0.00 ± 0.00
CoL_2	4.00 ± 0.20	0.00 ± 0.00	**12.10 ± 0.20**	**6.00 ± 0.20**	0.00 ± 0.00
NiL_2	0.00 ± 0.00	0.00 ± 0.00	0.00 ± 0.00	0.00 ± 0.00	**4.00 ± 0.40**
Ketoconazole	46.30 ± 0.40	40.00 ± 0.40	48.50 ± 0.40	48.00 ± 0.30	44.30 ± 0.40

Active when the diameter of the zone of inhibition is ≥ 6.00 ± 0.20 mm

Table 8. Diameters of the zone of inhibition on Bacteria

	Bacteria				
Samples	***E. coli***	***S. aureus***	***P. aeruginosa***	***E. faecalis***	***P.mirabilis***
H_2L_1	0.00 ± 0.00	0.00 ± 0.00	0.00 ± 0.00	0.00 ± 0.00	0.00 ± 0.00
CuL_1	**8.30 ± 0.40**	**10.30 ± 0.20**	0.00 ± 0.00	0.00 ± 0.00	0.00 ± 0.00
CoL_1	**10.50 ± 0.40**	**7.00 ± 0.40**	**6.50 ± 0.30**	0.00 ± 0.00	0.00 ± 0.00
NiL_1	0.00 ± 0.00	0.00 ± 0.00	0.00 ± 0.00	0.00 ± 0.00	**12.80 ± 0.20**
H_2L_2	**6.00 ± 0.40**	0.00 ± 0.00	0.00 ± 0.00	0.00 ± 0.00	0.00 ± 0.00
CuL_2	0.00 ± 0.00	0.00 ± 0.00	0.00 ± 0.00	0.00 ± 0.00	0.00 ± 0.00
CoL_2	**12.00 ± 0.30**	0.00 ± 0.00	**6.00 ± 0.20**	0.00 ± 0.00	0.00 ± 0.00
NiL_2	0.00 ± 0.00	0.00 ± 0.00	4.10 ± 0.20	0.00 ± 0.00	0.00 ± 0.00
Ciprofloxacin	28.80 ± 0.40	30.50 ± 0.40	26.00 ± 0.40	28.30 ± 0.30	30.00 ± 0.20

Active when the diameter of the zone of inhibition is ≥ 6.00 ± 0.20 mm

3.6.4. Minimum bactericidal concentration (MBC)

The minimum bactericidal concentrations of the compounds were determined by sowing 10 µL of the content of every well presenting no manifested change of color after revelation at the p-iodonitrotetrazolium chloride (INT). the chloride (INT). After sowing in the sterile boxes of Petri dish of 90 mm containing MHA, these boxes were incubated at 37 °C for 24 hours. At the end of the incubation, the smallest concentration underneath of which, no resumption of the bacterial growth was observed is the minimum bactericidal concentration and result are summarized in Tables 9.

The Schiff bases and their metal complexes

Table 9. Minimal inhibitory concentrations of the compounds (µg/ml)

Samples	Fungi										Bacteria									
	C. albicans		*C. glabrata*		*C. krusei*		*C. tropicalis*		*C. parapsilosis*		*E. coli*		*S. aureus*		*P. aeruginosa*		*E. faecalis*		*P.mirabilis*	
	MIC	MFC	MIC	MFC	MIC	MFC	MIC	MFC	MIC	MFC	MIC	MBC	MIC	MBC	MIC	MBC	MIC	MBC	MIC	MBC
H_2L_1	64	-	-	-	128	-	64	256	32	128	128	-	128	-	128	128	128	-	64	128
CuL_1	256	-	-	-	256	-		-		-	128	-	256	-	64	256	-	-		-
CoL_1	256	-	256	-	128	-	256	-	128	-	128	-	64	256	128	-	-	-	128	-
NiL_1	256	-	-	-		-		-	256	-	-	-	32	128	128	-	256	-	128	-
H_2L_2	256	-	-	-	256	-	256	-	256	-	64	256	32	128	128	-	-	-		-
CuL_2	256	-	-	-	256	-	256	-	256	-	-	-	128	-	256	-	-	-		-
CoL_2	128	-	128	-	128	-	128	-	128	-	128	-	64	256	32	128	256	-	128	-
NiL_2	256	-	-	-	256	-	256	-		-	-	-	256	-	128	-	-	-	256	-
Ketoconazole	0.5	8	0.25	8	0.125	0.5	8	8	2	4										
Ciprofloxacin											2	8	1	4	2	8	1	4	2	8

(-) means that the concentration are >256 µg/mL

3.10.1. Minimum fungicidal concentration (MFC)

The minimum fungicidal concentrations were obtained using the two-fold serial dilutions of compounds prepared in 96-well micro titre plates inoculated with 100 µL suspension containing colony-forming units at 37 ◦C for 48 hours. The lowest concentrations that induced an absence of turbidity at the bottom of the wells after incubation were noted as the minimum fungicidal concentrations and result are also summarized in Tables 9. The activities of compounds are considered significant when (MIC and MFC or MBC < 10 µg/mL), moderate when (10 ≤ MIC and MFC or MBC ≤ 256 µg/mL) and weak when (MIC and MFC or MBC > 256 µg/mL) Kuete *et al.,* (2010) [50].

It is observed from the biological data that, the Schiff bases and all complexes presents higher concentrations to inhibit microbial species, this indicated their weak antifungal and antimicrobial activities when compared to the standards used. However, CoL_1 and NiL_1 complexes are moderately active against *Staphylococcus aureus, Pseudomonas aeruginosa* and *Proteus mirabilis*, while CuL_1 complex is moderated active only against *Pseudomonas aeruginosa* when compared to the ligand H_2L_1. CoL_2 complex shows moderate activities against all tested species when compared to the ligand H_2L_2

3.11. Antioxidant activity of the Schiff base and its metal complexes

were screened for free radical scavenging activity by DPPH method using Trolox as a standard by measuring radical scavenging effect on DPPH radicals and the IC_{50} values. The results of the free radical scavenging activity of the compounds at different concentrations are shown in Figure 15.

It is evident from the results that the free radical scavenging activities of these compounds are concentration dependent [49, 52, 53]. Among the examined compounds, all the metal complexes exhibited higher scavenging activity than the Schiff bases. The marked antioxidant activity of the metal complexes, in comparison to free Schiff bases, could be due to the coordination of metal ions usinf the azomethine nitrogen of the ligands, and the oxygen atom of phenoxyl and naphtoxyl moieties. In case of the above test compounds, the hydrogen of azomethine is more acidic hence could easily be donated to the DPPH free radical and convert itself into the stable free radical [52, 53]. Figure 16 represent the histogram of IC_{50} values for H_2L_1 and H_2L_2 and their corresponding metal complexes for 50 % of DPPH radical.

$CoL_1$and CuL_1 complexes show good IC_{50} values compared to the ligand H_2L_1, while CoL_2, NiL_2 and CuL_2 show good IC_{50} values when compared to the ligand H_2L_2. This results affirms the fact that complexation increase the antioxidant activity [49, 52, 53]. Metal complexes of H_2L_1 Schiff base shows good IC50 values compared to complexes of the H_2L_2 Schiff base, this can be due to the steric effect of the ligand.

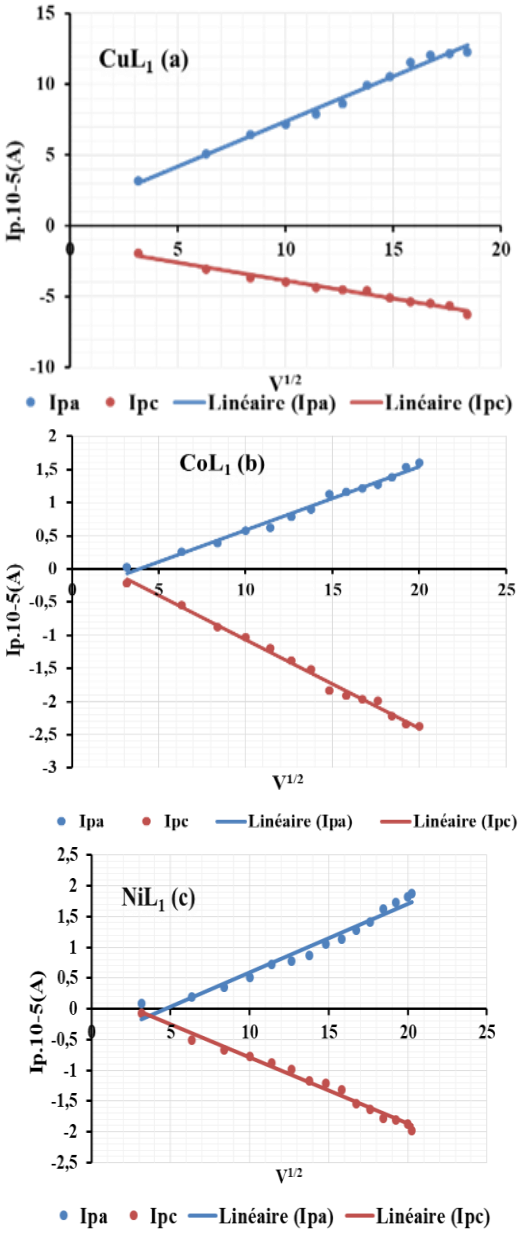

Figure 13. Plot of I_p vs. $v^{1/2}$ for (a) $Cu(II)L_1$, (b) $Co(II)L_1$ and (c) $Ni(II)L_1$ complexes

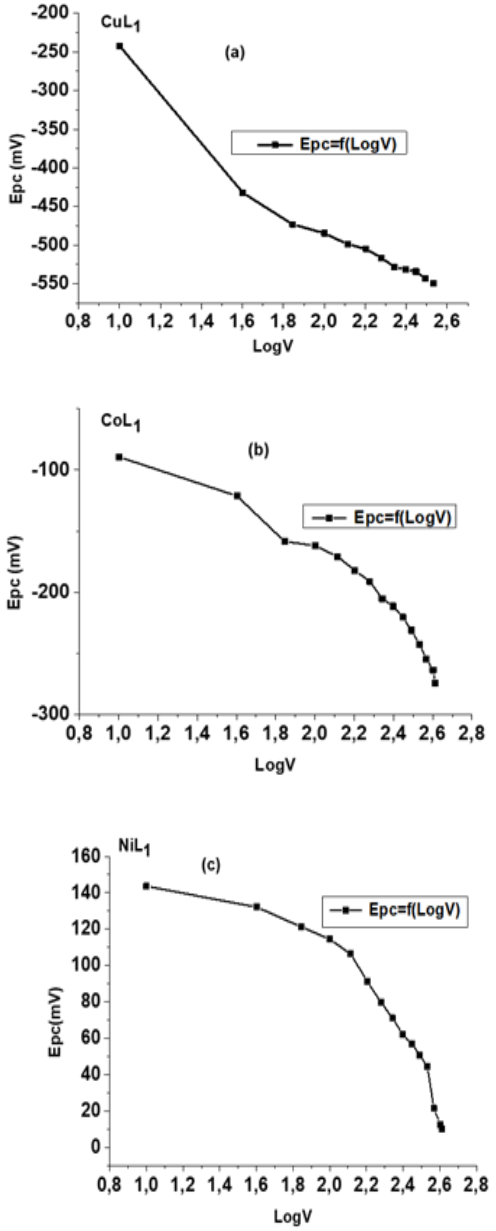

Figure 14. Plot of E_{pc} vs. LogV for (a) $Cu(II)L_1$, (b) $Co(II)L_1$ and (c)

4. Conclusion

We have prepared and characterized two new tetradentate Schiff base ligands (H_2L_1 and H_2L_2), which coordinate easily to Co(II), Cu(II) and Ni(II) ions to form tetrahedral Cobalt and Nickel complexes, and square planar Copper complexes. Cyclic voltammetry studies of the ligand and their metal complexes reveal that the redox systems Co(III)/Co(II) and Ni(III)/Ni(II) displayed quasi-reversible processes while Cu(III)/Cu(II) displayed an irreversible process.

Substituents have a detectable effect on the electrochemical behaviour of the Schiff bases and their complexes. Significant correlations have been observed between redox potentials and antioxidant properties. It is found that compounds with strong scavenging capabilities are oxidized at relatively low potentials and therefore the oxidation potentials can be used as a general indicator of radical scavenging ability. Knowledge of the electronic and steric effects that control redox processes of these compounds offers very interesting research opportunities and may

be critical in the design of new research projects. Antibacterial studies show moderate activity of the compounds with the complexes being more active than the free ligand on some bacterial and fungal strains thus confirming that chelation can increase antimicrobial activity.

Conflict of interest

The authors declare that there are not conflicts of interest.

Data Availability

All the data used to support the findings of this study are included within the article. Any other data are available from the corresponding author upon request.

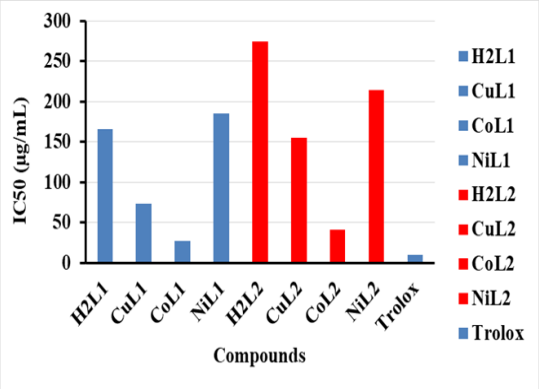

Figure 16. IC_{50} values for H_2L_1 and H_2L_2 and their corresponding metal complexes for 50 % of DPPH radical comparison was made against Trolox

Funding

This work was partly funding under the *'Fond de modernisation et d'appui a la recherche'* allocation to Higher Education University Teachers of Cameroon.

Acknowledgment

The authors acknowledge the Dr NGOMPE M. Gustave Eric of the Organic Chemistry Department of the University of Yaounde I for ^{1}H MNR and ^{13}C MNR analysis.

References

[1]. Segura J.L, Mancheño M.J, Zamora F. Covalent organic frameworks based on Schiff-base chemistry: Synthesis, properties and potential applications. *Chemistry Society Review*. 2016. 45: 5635–5671.

[2]. Nica, S, Rudolph M, Lippold I, Buchholz A, Görls H, Plass W. Vanadium(V) Complex with Schiff-Base Ligand Containing a Flexible Amino Side Chain: Synthesis,

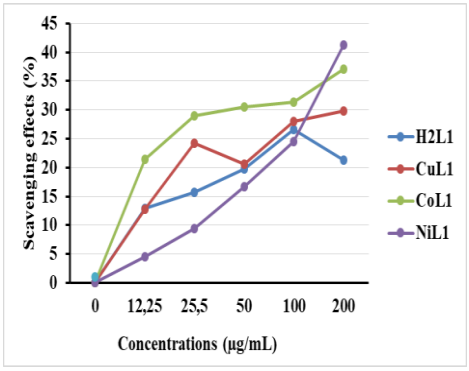

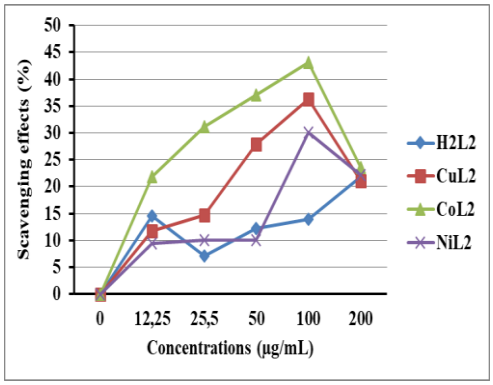

Figure 15. DPPH radical scavenging activity of H_2L_1; H_2L_2 and their corresponding metal

Structure and Reactivity. *Journal of Inorganic and. Biochem*istry. 2015.147: 193-203.

[[3]. Akitsu, T. and Einaga, Y. Synthesis and Crystal Structures of the Flexible Schiff Base Complex Bis(N-1,2-Diphenylethyl-Salicydenaminato-κ2N,O) Copper(II) (Methanol): A Rare Case of Solvent-Induced Distortion. *Polyhedron*. (2006) 25: 1089-1095.

[4]. Al Zoubi. W., Ko. Y.G., Schiff base complexes and their versatile applications as catalysts in oxidation of organic compounds: Part I. *Appl. Organometallic Chemistry*. (2016).31:

[5]. Sarkar. S., Jana. M., Mondal. T., Sinha. C.,. Ru-halide-carbonyl complexes of naphthylazoimidazoles; synthesis, spectra, electrochemistry, catalytic and electronic structure. *J. Organomet. Chem.*, (2012). *716*: 129–137.

[6]. Dikio. C. W., Okoli. B. J., Mtunzi. F. M. Synthesis of new anti-bacterial agents: Hydrazide Schiff bases of vanadium acetylacetonate complexes. *Cogent Chemidtry*. (2017).3: 4-14.

[7]. Malik S., Nema. B., (2016). Antimicrobial activities of Schiff Bases: A review., *International Journal of Theorical and Applied Sciences*. (2016).8(1): 28-30.

[8]. Siva. C., Silva. D., Modolo. L., Alves. R., Rwsende. M., Martins. C., Fatima. A. Schiff

bases: A short review of their antimicrobial activities. *Journal of Advance Research.*. (2011). 2: 1–8.

[9]. Shubhangi N. K., Harjeet D. J. Synthesis, Characterization, and Antimicrobial Studies of N, O Donor Schiff Base Polymeric Complexes. *Hindawi Journal of Chemistry.* (2013) .2013:1-5

[10]. Malik. M. A., Dar. O. A., Gull. P., Wani. M. Y., Hashmi. A. A. Heterocyclic Schiff Base Transition Metal Complexes in Antimicrobial and Anticancer chemotherapy. *Med. Chem. Commun.*. (2017). 2017: 1-75

[11]. Jian L., Tingting L., Sulan C., Xin W., Lei L., Yongmei W.,. Synthesis, structure and biological activity of cobalt (II) and Copper (II) complexes of valine-derived Schiff bases. *Journal of Inorganic and. Biochem*istry. (2006).100: 1888–1896.

[12]. Vidya Rani, C., Kesavan, M.P., Haseena, S.., Bidentate Schiff Base Ligands Appended Metal(II) Complexes as Probes of DNA and Plasma Protein: In Silicon Molecular Modelling Studies. *Appl Biochem Biotechnol*. (2020). 191: 1515–1532.

[13]. Tümer, M., Çelik, C., Köksal, H. Mehmet.; Selahattin Serin. Transition metal complexes of bidentate Schiff base ligands. *Transition Metal Chemistry* (1999), 24: 525–532.

[14]. Ikechukwu P. Ejidike, Peter A. Ajibade, "Synthesis, Characterization, Anticancer, and Antioxidant Studies of Ru(III) Complexes of Monobasic Tridentate Schiff Bases", *Bioinorganic Chemistry and Applications*, 2016, 11 pages, 2016. doi.org/10.1155/2016/9672451

[15]. Roberto C. Felicio, Gislaine A. da Silva, Lucinéia F. Ceridorio and Edward R. Dockal. Tetradentate Schiff Base Copper(II) Complexes, *Synthesis and Reactivity. Inorganic and Metal-Organic Chemistry*, (1999) 29(2): 171-192,

[16]. Saranya, J., Jone Kirubavathy, S., Chitra, S. *et al.* Tetradentate Schiff Base Complexes of Transition Metals for Antimicrobial Activity. *Arabian Journal of Sciences and Engineering* (2020). 45: 4683–4695.

[17]. Aida L. El-Ansary, Hussein M. Abdel-Fattah & Nora S. Abdel-Kader Synthesis and characterization of tetradentate ***bis*** -Schiff base complexes of di- and tri-valent transition metals, *Journal of Coordination Chemistry.* (2008). 61: 2950-2960,

[18]. Sreenivas V., Srikanth G., Aruna M., Vijaya K. P., Muralidhar R. P., Ravinder V. Synthesis, Characterization and Antibacterial Activity and DNA cleavage Studies of tetra dentate Schiff bases and their Zn (II) Complexes., *Research. Journal of Chemistry and. Sciences.* (2014).4(6); 66-72

[19]. Bahaffi S. O., Abdel Aziz A., El-Naggar M. M.. Synthesis, spectral characterization, DNA binding ability and antibacterial screening of copper(II) complexes of symmetrical NOON tetradentate Schiff bases bearing different bridges., *Journal of Molecular Structure*. (2012). 1020: 188–196.

[20]. Asadi M., Sepehrpour H., Mohammadi K. H. Tetradentate schiff base ligands of 3,4-diaminobenzophenone: synthesis, characterization and thermodynamics of complex formation with Ni(II), Cu(II) and Zn(II) metal ions. *Journal of the Serbian Chemical Society*. (2011).76: 63–74.

[21]. Praveen k. S, Metal complexes of cobalt(II), nickel(II), copper(II) and zinc(II) with N-(2-hydroxy-l-naphthylidene)-L-amino acids, *Proc. Indian Academic sciences(chemical Sciences)*. (1994). 106: 23-27

[22]. Kuate M., Conde M.A., Mainsah N. E., Paboudam A.G., Tchieno F. M., Ketchemen K. I. Y., Kenfack T. I., Ndifon P.T. Synthesis, Characterization, cyclic voltammetry and biological Studies of Co(II), Ni(II), and Cu(II) Complexes of a tridentate Schiff base 1-((E)-(2-mercaptophenylimino) methyl) naphthalen-2-ol(H_2L_1)., *Hindawi. Journal of Chemistry*. (2020). 2020: 1-21.

[23]. Kuate M., Conde M.A., Nchimi K.N., Paboudam A.G., Ntum S.-J.E., Ndifon P.T. Synthesis, Characterization and Antimicrobial Studies of Co(II), Ni(II), Cu(II) and Zn(II) Complexes of (E)-2-(4-Dimethylbenzydimino)-Glycylglycine, (Glygly-DAB) a Schiff Base Derived from 4-Dimethylaminobenzaldehyde and Glycylglycine. *International Journal of Organic Chemistry*. (2018). 8: 298-308.

[24]. Ntum, S.-J.E., Paboudam, A.G., Conde, A.M., Nyamen, L.D., Mohamadou, A., Raftery, J. and Ndifon, P.T. Synthesis and Crystal Structure of N-(2-Pyridylmethyl)-L-Alanine) Isothiocyanate Cobalt (III). *Crystal Structure Theory and Applications*. (2017).6: 39-56.

[25]. Bharati. K.T., Gujarathi D.B., Tryambake P.T., Hase G.J., Gaikwad R.K., Khatal M.B., Preparation of Schiff base of 1, 2, 4-Triazole-4-amine with 3-Nitrobenzaldehyde, Its Complexation with Cu (II) and Zn (II) and Antimicrobial Activity of Complexes., *Der Chemica Sinica*. (2017). 8(2): 223-228

[26]. Garcia E. J., Oldoni T. L., De Alencar S. M., Reis A., Loguercio A. D., Grande M. R. Antioxidant Activity by DPPH Assay of Potential Solutions to be Applied on Bleached Teeth., *Braz. Dent .J*. (2012). 23(1): 22-27

[27]. Mensor L., Boylan F., Reis A., Leitao G. Screening of Brazilian plant extracts for antioxidant activity by the use of DPPH free radical method. *phythotherapy Research.*, (2001).15(2): 127-30.

[28]. Jaslin E., Padmaja V., Antioxidant properties and total phenolic content of ethanolic extract of aerial parts of Coleus spicatus. Benth. *Journal of Pharmaceutical Research*. (2011).4(5): 1363-1364

[29]. Balachandar B., Jayachitra A., Paramasivam S.; Arulkumar A. Evaluation of Antioxidant Activity of *Clitoria ternatea* and *Alternanthera sessilis* Plant Extracts Using Model System for Yeast Cells. *African Journal Basic. Applied. Sciences.* (2013)..5 (3):134-138

[30]. Berghe V., Wietinck A. Screening methods for antibacterial and antiviral agents from higher plants. *Meth. Plant Biochem*. (1991).6, 47-68

[31]. Newton S., Lau C., Gurcha S., Besra G., Wright C. The evaluation of forty-three plant species for in vitro antimycobacterial activities; isolation of active constituents from Psoralea corylifoliaand *Sanguinaria Canadensis Journal Ethnopharmacol*. (2002).79: 57–63

[32]. Kiehlbauch J., Hannett G., Salfinger M., Wendy A., Monserrat C., Carlyn. Use of the National Committee for Clinical Laboratory Standards Guidelines for Disk Diffusion Susceptibility Testing in New York State Laboratories, *J. Clin. Microbiology*, (2000). 38 (9): 3341–3348

[33]. Tereshuck M., Riera M., Castro G., Abdala L. Antimicrobial Activity of Flavonoid from Leaves of Tagetes Minuta. *Journal of Ethnopharmacol*. (1997).56, 227-232.

[34]. Sreenivas V., Aruna M., Ravinder V. Synthesis and Spectral Characterization of tetra dentate Schiff bases and their Zn (II) Complexes., *Journal of Chemical and Pharmaceutical Sciences*. (2014). 5: 8-10

[35]. Murlidhar R., Gaurav P., Amit Y., Anand A. Synthesis, Spectral Characterization and Antimicrobial Studies of some Transition Metal Complexes with ONNO-donor tetradentate ligand., *Research Journal of Pharmaceutical,. Biological and Chemical Sciences*. (2011). 2(3): 341-347

[36]. Amani S. A., Abdel-Nasser M. A., Reda A., Mohamed E. Z. Synthesis, Spectral Characterization, and Thermal and Cytotoxicity Studies of Cr(III), Ru(III), Mn(II), Co(II), Ni(II),Cu(II), and Zn(II) Complexes of Schiff Base Derived from 5-Hydroxymethylfuran-2-carbaldehyde. *Hindawi. Journal of Chemistry*. (2018).2018: 1-17

[37]. Afaq A.T. Synthesis and Characterization of Some New Schiff Base Derivatives from 4-Nitro-*o*-Phenylene diamine. *Journal of kerb. univ*., (2013). 10(3): 259-266.

[38]. Al-Nuzal S. M., Al-Amery A., Synthesis, Characterization, Spectroscopy and Bactericidal Properties of Polydentate Schiff Bases Derived from Salicylaldehyde and Anilines and their Complexes., *Journal of Chemical and Pharmaceutical Reseach.*. (2016). 8(11): 290-301

[39]. Selma Y., Mustafa U., Synthesis and Characterization of New Schiff Bases and Their Cobalt(II), Nickel(II), Copper(II), Zinc(II), Cadmium(II) and Mercury(II) Complexes, Synthesis and Reactivity in Inorganic, *Metal-Organic and Nano-Metal Chemistry,* (2005). 35: 417-421

[40]. Abdallah S. M., Zayed M.A., Mohamed G. Synthesis and spectroscopic characterization of new tetradentate Schiff base and its coordination compounds of NOON donor atoms and their antibacterial and antifungal activity., *Arabian. Journal of Chemistry*. (2010). 3:103–113

[41]. Neelakantan. M. A., Rusalraj F., Dharmaraja J., Johnsonraja S., Jeyakumar T., Sankaranarayana P. M., Spectral characterization, cyclic voltammetry, morphology, biological activities and DNA cleaving studies of amino acid Schiff base metal(II) complexes., Spectrochimica Acta Part A, (2008) 71: 1599–1609

[42]. Bagihalli G. B., Avaji P. G., Patil S. A., Badami P. S. Synthesis, spectral characterization, in vitro antibacterial, antifungal and cytotoxic activities of Co(II), Ni(II) and Cu(II) complexes with 1,2,4-triazole Schiff bases., *Europeen Journal of Medicinal Chemistry*. (2008). 43: 2639-2649.

[43]. Zolezzi S., Spodine E., Decinti A. Electrochemical studies of copper(II) complexes with Schiff base ligands, *Polyhedron*.. (2002). 21: 55–59

[44]. Shaju K., Joby T.,Vinod P., NimmyKuriakose. Spectral and Cyclic Voltammetric Studies on Cu(II)-Schiff Base Complex Derived from Anthracene-9(10 H)-one, *IOSR Journal of Applied Chemistry*. (2014). 7(10): 64-68.

[45]. Aburas N., Lolic A., Stevanovic N., Tripkovic T., Mandic S. N., Rada B. Electrochemical behavior and antioxidant activity of tetradentate Schiff bases and their copper(II) complexes. *Journal of the Iranian Chemical. Society*. (2012). 2012: 1-5

[46]. Hoda A. B., Abdel-Nasser M.A., Mutlak S. A., Cu(II), Ni(II), Co(II) and Cr(III) Complexes with N_2O_2-Chelating Schiff's Base Ligand Incorporating Azo and Sulfonamide Moieties: Spectroscopic, Electrochemical Behavior and Thermal Decomposition Studies. *International Journal of Electrochemical Sciences.*(2013). 8: 9399 - 9413

[47]. Larabi L., Harek Y., Reguig A., Mostafa M. M., Synthesis, structural study and electrochemical properties of copper(II) complexes derived from benzene- and *p*-

toluenesulphonylhydrazones. *Journal of the Serbian Chemical Society*. (2003). 68(2): 85–95

[48]. Feng X., Song H., Huo S. Synthesis, Crystal Structure and Electrochemistry Properties of a Cobalt(II) Complex Based on Asymmetry Schiff Base Ligand. *Chinese Journal of Structural Chemistry*. (2014). 33(6): 897─902

[49]. Rajavel R., Akila E., Usharani M. Metal (II) Complexes Of Bioinorganic And Medicinal Relevance: Antibacterial, Antioxidant And Dna Cleavage Studies Of Tetradentate Complexes Involving O, N-Donor Environment Of 3, 3′-Dihydroxybenzidine-Based Schiff Bases., *International Journal of Pharmacy and Pharmaceutical Sciences*.(2013). 5(2): 573-581

[50]. Kuete V., Ngami B., Tangmouo J., Bola J., Ngadjui B. Efflux pumps are involved in the defence of gram negitive bacterial against the natural products isobvachalcone and diospyrone, *Antimicrobial Agents and chemotherapy*. (2010). 54: 1749-1752.

[51]. Priyadarshini G., Namitha R., Mageswari D., Selvi G. Synthesis Characterization and Antioxidant Activity of Ni (II) and Co (II) Quinoline Schiff Base. *International Journal of Innovative Research in Science, Engineering and Tech*nology. (2016). 5 (1): 101-107.

[52]. Mahendra R. K., Vivekanand B., Mruthyunjayaswamy B. H. M. Synthesis, Characterization, Antimicrobial, DNA Cleavage, and Antioxidant Studies of Some Metal Complexes Derived from Schiff Base Containing Indole and Quinoline Moieties., *Hindawi Bioinorganic Chemical Applied.* (2018). 2013: 1-16

[53]. Raja J. D., Senthilkumar G. S., Vedhi C., Vadivel M.. Synthesis, structural characterization, electrochemical, biological, antioxidant and nuclease activities of 3-morpholinopropyl amine mixed ligand complexes., *Journal of Chemical and Pharmaceutical Research*.. (2015).7(10): 1-14